Polyhedron 136 (2017) 117–124

Contents lists available at ScienceDirect

Polyhedron

journal homepage: www.elsevier.com/locate/poly

Cu(II)–Gd(III) 2D-coordination polymer based on two different organic linkers

Carlos Cruz [a,b], Evgenia Spodine [a,b], Diego Venegas-Yazigi [b,c], Verónica Paredes-García [b,d,*]

[a] Universidad de Chile, Facultad de Ciencias Químicas y Farmacéuticas, Departamento de Química Inorgánica y Analítica, Chile
[b] CEDENNA, Chile
[c] Universidad de Santiago de Chile, Facultad de Química y Biología, Departamento de Ciencias de los Materiales, Chile
[d] Universidad Andres Bello, Facultad de Ciencias Exactas, Departamento de Ciencias Químicas, Chile

ARTICLE INFO

Article history:
Received 30 December 2016
Accepted 6 February 2017
Available online 14 February 2017

Keywords:
3*d*–4*f* heterometallic networks
Cu(II)–Gd(III) coordination polymer
Ferromagnetic behaviour
2d covalent networks
Two step synthesis

ABSTRACT

A new Cu^{II}–Gd^{III} heterometallic coordination polymer was obtained by a two-step synthesis, using the molecular complex $[Cu(H_2IDC)_2(2,2'\text{-bipy})]\cdot 2H_2O$ (**1**) as metalloligand and oxalate as auxiliary ligand (H_3IDC = 1H-imidazole-4,5-dicarboxylic acid). The new extended heterometallic network $[Gd(H_2O)_2(C_2O_4)Cu(IDC)]\cdot H_2O$ (**2**) crystallizes in a $P\bar{1}$ triclinic space group presenting a 2D covalent structure. From a structural point of view, (**2**) can be defined as Gd-zigzag chains $[Gd(H_2O)_2(C_2O_4)]^+$ linked by Cu-based molecules, $[Cu(IDC)]^-$. A 3D structure is reached by non-covalent interactions between the layers. Also Gd···Cu interlayer interactions through *syn–anti* carboxylate ligands can be observed. Whereas, from room temperature to 100 K the network behaves as a paramagnet, below 20 K ferromagnetic interactions are observed. The ferromagnetic state was also corroborated by isothermal hysteresis loops measured at 2 K, giving values for H_c and M_r of 50 Oe and 500 emumol^{-1}, respectively.

1. Introduction

In recent years, coordination polymers (CPs) have gained much attention mainly by the intriguing architectures, topologies, and by the promising chemical and physical properties they present [1–5]. Thus, heterometallic coordination polymers (HCPs) including two different kind of metal cations, 3*d* and 4*f*, are also a flourishing research field. The structural richness and properties such as, chirality, magnetism or luminescence have made HCPs a subject of intensive research [6–8]. The assembly of the HCPs is mainly reached by two different synthetic approaches. The one step synthesis considers the mixture of both organic and inorganic reagents at the same time, while in the second approach, a molecular 3*d* metalloligand is previously synthesized, reacting later with the 4*f* cation to give the 3*d*–4*f* HCPs. From a synthetic point of view, Cu^{II}-4*f* HCPs are attractive due to the coordination plasticity of Cu^{II} ions, which should produce a wide variety of coordination networks [9]. As an example, Cu^{II} complexes with Schiff-bases [7] or with oxamides [10,11] have proven to be effective metalloligands in the synthesis of polynuclear heterometallic Cu^{II}-4*f* complexes. Moreover, Schiff-bases functionalized with carboxylic groups have also been used to obtain one dimensional Cu^{II}-4*f* coordination polymers, being the 4*f* cations linked by carboxylate bridges [12]. Additionally, complexes synthesized from Cu^{II} cations and malonamide-*N*,*N*′-diacetic acid as ligands, give Cu^{II}-4*f* 2D networks, where the carboxylate groups also promote the incorporation of 4*f* cations in the structures [13]. On the other hand, interesting properties displayed by Cu^{II}–Gd^{III} HCPs have also been reported by Ye et al., for $[Gd_2Cu(NIPH)_4(H_2O)_4]\cdot 6H_2O$ where NIPH = 5-nitroisophthalate. These authors reported a reversible single-crystal to single-crystal transformation, based on a dehydration and rehydration process of the porous framework [14]. Besides, Miao et al., reported a relatively large magnetocaloric effect for the 1D HCP, $[CuGd(pta)_2(Hpta)(4,4'\text{-bipy})_{0.5}(H_2O)]$ with H_2pta = phthalic acid, as a consequence of the ferromagnetic interaction between the spin carriers present in the $[Cu_2Gd_2]$ moieties, and also because of the lack of magnetic anisotropy of both cations [15].

Literature data shows that multidentate ligands exhibiting flexible coordination modes with metal ions are useful in the construction of CPs. In this sense, different three-dimensional frameworks based on lanthanide-zinc ions have been synthesized via hydrothermal reaction. While $\{[Ln_2(H_2O)_2Zn_4(H_2O)_4(ImDC)_4(ox)]6H_2O\}_n$ (Ln = La, Nd, Sm, Eu) were obtained using 1H-imidazole-4,5-dicarboxylic acid and oxalic acid as ligands [16], $[H(H_2O)_8][LnZn_4(imdc)_4(Him)_4]$ (Ln = La, Pr, Eu, Gd, Tb) were obtained using 1H-imidazole-4,5-dicarboxylic acid and imidazole (Him) as the

* Corresponding author at: Universidad Andres Bello, Facultad de Ciencias Exactas, Departamento de Ciencias Químicas, Chile.
E-mail address: vparedes@unab.cl (V. Paredes-García).

http://dx.doi.org/10.1016/j.poly.2017.02.002
0277-5387/

secondary ligand [17]. Despite that much work has been developed in these systems, the synthesis and characterization of new Cu^{II}–Gd^{III} complexes enriches the chemistry involved in the 3*d*–4*f* heterometallic networks, aiming also for a better understanding of the nature of the different observed properties. In this sense, we are reporting the structural and magnetic characterization of a new 2D Cu^{II}–Gd^{III} HCP $[Gd(H_2O)_2(C_2O_4)Cu(IDC)]\cdot H_2O$ (**2**), which was obtained from a copper-metalloligand synthesized from 1H-imidazole-4,5-dicarboxylic acid (H_3IDC) and 2,2′-bipyridine, $[Cu(H_2IDC)_2(2,2bipy)]\cdot 2H_2O$ (**1**). Taking into account the multiple deprotonation degrees that the H_3IDC ligand can acquire giving species such as H_2IDC^-, $HIDC^{2-}$, IDC^{3-} and the wide capability to bind multiples metal centres, we consider that 1H-imidazole-4,5-dicarboxylic acid is an exceptional and efficient organic ligand to obtain not only extended structures but also new 3*d*–4*f* HCPs.

2. Materials and methods

2.1. Single-crystal X-ray diffraction

Single crystals of compounds (**1**) and (**2**) were directly picked from the reaction vessel, and glued on the tip of a capillary glass using epoxy resin. Quick scans on the Bruker APEXII diffractometer confirmed enough crystal quality to perform full recording of both compounds. Data were reduced by SAINT [18], and empirical absorption correction were applied using SADABS [19]. Using the OLEX2 [20] package, the structure was solved with the SHELXT [21] structure solution program using Direct Methods and refined with the SHELXL [22] refinement package using Least Squares minimisation. Additional data concerning the crystals and the refinement parameters are detailed in the Supporting information (Table S2).

2.2. Magnetic susceptibility

Magnetic measurements were carried out using a Quantum Design Dynacool Physical Properties Measurement System (PPMS), equipped with a Vibrating Sample Magnetometer (VSM). The *dc* data were collected under external applied fields of 0.2, 0.5 and 1 kOe in the 2–300 K temperature range. Diamagnetic corrections (estimated from Pascal constants) were considered [23]. Magnetization measurements were performed between 0 and ±90 kOe at temperatures varying from 2 to 11 K. Alternating current (*ac*) magnetic susceptibility measurements were performed on (**2**) at 1.25 kOe-*dc* field and a 4 Oe oscillating field, in the frequency range of 178 and 1000 Hz.

2.3. Spectroscopic measurements

FTIR spectra were recorded on a Perkin Elmer BX-II spectrophotometer in the 4000–400 cm^{-1} range, using KBr pellets. UV–Vis-NIR spectra were obtained on a Perkin Elmer Lambda 1050 spectrophotometer UV–Vis/NIR, equipped with a Perkin Elmer 150 mm InGaAs Integrating sphere. The measurements were carried out in the 200–1200 nm range using the solid sample without any support.

2.4. Thermogravimetric measurements

Thermal gravimetric analysis was performed on a Mettler Toledo TGA/DSC STAR system using N_2 atmosphere. The samples were introduced in an alumina holder and heated from room temperature to 900 °C with a rate of 5 °C/min.

3. Experimental

3.1. Synthesis of $[Cu(H_2IDC)_2(2,2bipy)]\cdot 2H_2O$ (1)

All reagents and solvents used to obtain (**1**) and (**2**) were of p.a. quality, and used without any previous purification process. A suspension in continuous stirring of H_3IDC (0.156 g, 1.00 mmol), 2,2-bipyridine (0.078 g, 0.50 mmol) and 70 μL of dipropylamine (DPA) in 10 mL of acetonitrile (MeCN), was mixed with a solution of $Cu(NO_3)_2\cdot 3H_2O$ (0.121 g, 0.50 mmol) in 10 mL of H_2O/MeCN 1:1. The deep blue slurry solution was filtered and the supernatant was kept at room temperature for 1 day providing blue needle-like crystals, which can be isolated by filtration. As the crystals turned opaque under air suggesting a loss of crystallinity, for X-ray experiments the crystals were picked out and immediately glued to avoid any solvent loss. MW: 565.9 g/mol. Yield of 82%, based on copper salt.

3.2. Synthesis of $[Gd(H_2O)_2(C_2O_4)Cu(IDC)]\cdot H_2O$ (2)

Compound (**2**) was obtained in a two steps reaction, using (**1**) as metalloligand. (**1**) (0.053 g, 0.10 mmol), $Gd(NO_3)_2\cdot 6H_2O$ (0.090 g, 0.20 mmol) and $K_2C_2O_4\cdot H_2O$ (0.037 g, 0.2 mmol) were placed in a 23 mL Teflon-lined stainless steel autoclave vessel with 10 mL of water and heated at 120 °C under self-generated pressure for 5 days. The reaction mixture was naturally cooled down to room temperature; light blue plate crystals of (**2**) stable and suitable for X-ray diffraction were separated by filtration. PM: 515.96 g/mol. Yield of 38.5%, based on lanthanide salt.

4. Results and discussion

4.1. Synthesis

According to a previous work, we used the 1H-imidazole-4,5-dicarboxylic acid (H_3IDC) ligand due to its outstanding coordination capabilities to create intricate 4*f* homometallic networks [24,25] and also structures presenting helical chain arrangements [26,27]. From a synthetic point of view, $[Cu(H_2IDC)_2(2,2bipy)]\cdot 2H_2O$ (**1**) is a promising metalloligand for the synthesis of 3*d*–4*f* heterometallic materials. In the previous reported Co^{II}–Gd^{III} network [28], the $[Co(H_2IDC)_2(H_2O)_2]$ metalloligand was used together with oxalate as secondary ligand and the lanthanide cation to obtain a 3D network. In the present study, we used 2,2-bipyridine (2,2-bipy) as secondary ligand in (**1**) to modulate the dimensionality of the network, by blocking two coordination sites of the Cu^{II} centre. However, when (**1**) was put under hydrothermal conditions to obtain (**2**), the 2,2′-bipy ligand is lost and therefore not present in the synthesized HCP (**2**). Even though the initial ratio between Cu and Gd cations was 1:2, under the used solvothermal conditions the thermodynamically more stable compound with a 1:1 molor ratio between both cations was obtained. Noticeably, if a 1:1 ratio between the metal cations is used as initial condition, $[Gd(H_2O)_2(C_2O_4)Cu(IDC)]\cdot H_2O$ (**2**) is not produced.

4.2. Thermogravimetric behaviour (TG)

The thermal stability of (**2**) was tested under N_2 atmosphere (Fig. S1). The thermogram of (**2**) shows a first weight lost between 150–270 °C corresponding to 10.4%. This value correlates well with the expected loss of all water molecules, associated with two coordinated and one crystallization ones (10.5%) to give a anhydrous compound $[Gd(C_2O_4)Cu(IDC)]$. Later three consecutive steps occur, giving a weight loss of 14.0%, 17.0% and 15.3% at 320 °C, 440 °C and 720 °C respectively (Table S1). The value of 14.0% matches well

with the release of the imidazole fragment, C_3HN_2 (14.0%), as product of the degradation of IDC^{3-} fragment. Although De Moura et al. have reported for complexes based on Cd^{II}, bromide and imidazole, the loss of imidazole molecules at temperatures above 370 °C, [29] it is also clear that in our case, complementary analysis should be done to confirm the loss of the imidazole fragment. The final two steps, between 440 °C and 720 °C, should correspond to the total decomposition of (**2**).

4.3. Spectroscopic behaviour

FTIR of (**1**) and (**2**) are given in Fig. S2. A broad band in the range of 3700–3100 cm^{-1} is assigned to stretching vibrations (ν_{O-H}) of water molecules. Strong and broad absorption associated to asymmetric ($\nu_{COOasym}$) and symmetric (ν_{COOsym}) vibrations of the carboxylate groups, belonging to the H_2IDC^- for (**1**) and IDC^{3-} and oxalate vibrations in (**2**), appear in the region of 1700–1300 cm^{-1}. The bands corresponding to the C=C and N=C bonds of imidazole ring and 2,2-bypiridine ($\nu_{C=C}$ and $\nu_{C=N}$), are found almost in the same region of the carboxylate groups, being overlapped with these stronger vibrations. The band associated to the protonated carboxylic group in H_2IDC^- in (**1**) should appear at 1700 cm^{-1} but is not observed probably due to its lower intensity due to the existence of H-bonds.

Electronic UV–Vis-NIR spectra of (**2**) and H_3IDC free ligand are shown in Fig. S3. Both spectra have strong absorptions below 400 nm, with a maximum at 255 and 320 nm assigned to π–π^* and n–π^* transitions of the organic ligand [30]. On the other hand, three *d*–*d* transitions corresponding to ν_1 ($d_{xz}/d_{yz} \rightarrow d_{x^2-y^2}$), ν_2 ($d_{xy} \rightarrow d_{x^2-y^2}$) and ν_3 ($d_{z^2} \rightarrow d_{x^2-y^2}$) can be expected for a Cu^{II} cation presenting a square planar geometry. While for [Cu(acac)$_2$] based complexes, absorptions at 500, 650 y 750 nm assigned to ν_1, ν_2 and ν_3, respectively were observed in the presence of a non-coordinating solvent [31], Kongchoo et al. reported only one absorption at 500 nm in solid state for a square planar Cu^{II} macrocyclic complex [32]. In our case $[Gd(H_2O)_2(C_2O_4)Cu(IDC)]\cdot H_2O$ (**2**) gives one wide absorption centred at 650 nm, being associated to the overlap of ν_1, ν_2 and ν_3 transitions [33]. Emission UV–Vis spectra in solid state for (**2**) were recorded at excitation energies associated to each maximum of the absorption spectra, but no emission was observed in the studied range.

4.4. Structural description

Structural parameters of (**1**) and (**2**) are given in Tables 1 and S2. Analysis of single crystal X-ray diffraction revealed that $[Cu(H_2IDC)_2(2,2bipy)]\cdot 2H_2O$, (**1**) crystallizes in a triclinic $P\bar{1}$ space group, and corresponds to a mononuclear complex where the Cu^{II} centre is in a four-coordinated environment CuN_4, giving a square planar geometry (Fig. S4). No counterion was found in (**1**), therefore, the charge balance suggests that the imidazole ligand is in a diprotonated form, H_2IDC^-, reported also in other similar molecular compounds [34–37]. In the structure of (**1**) the Cu^{II} centre is bonded to one bidentate $\kappa N,N'$-bipy and two κN-H_2IDC^- anions, with the Cu^{II} centres interacting through the axial position with the carboxylate groups belonging to the H_2IDC^- ligand. Furthermore, two water crystallization molecules were found. Considering that the solvent loss makes (**1**) very unstable outside the mother liquor, poor single crystal diffraction data were obtained. Therefore, the electronic density associated to solvent molecules (modelled as solvent mask) could not be assigned, obtaining an R factor ca.12%. However, the crystallographic data of (**1**) had enough quality to identify a well-defined mononuclear complex. This information allows us to examine the changes in the coordination around the Cu^{II} centres when this metalloligand is used to give the HCP (**2**).

The analysis of the single crystal X-ray diffraction for compound (**2**) shows an extended 2D covalent network presenting an asymmetric unit formed by one Cu^{II} and one Gd^{III} cations, one full-deprotonated IDC^{3-} ligand, one oxalate anion ($C_2O_4^{2-}$) and three water molecules (Fig. 1a). The layers are further connected though H-bonds, reaching a 3D structure (Fig. 1b). The Cu^{II} cation presents a square planar geometry with a CuN_2O_2 coordination sphere, formed by two bidentate $\kappa N,O$-IDC^{3-} ligands coordinated in a *trans* conformation. Also, Cu^{II} interacts in the axial position with two additional free carboxylate groups belonging from another two IDC^{3-} molecules (Cu—O = 2.577(5) Å), thus forming an elongated octahedron. The axial and equatorial IDC^{3-} molecules have the planar imidazole rings disposed in a parallel form, permitting a π–π staking interaction among them (Fig. 2a). In other Cu^{II}–Gd^{III} polymers based on pyridine-2,3-dicarboxylic acid [38] or pyridine-2,5-dicarboxylic acid [39] a similar parallel arrangement can be found between the axial and equatorial ligand rings.

An eight-coordination around the Gd^{III} is observed, reached exclusively by oxygen atoms, belonging to one O,O'-IDC^{3-}, two independent chelating O,O'–$C_2O_4^{2-}$, and two water molecules. The geometry on Gd^{III} was confirmed by the SHAPE software, obtaining the more accurate fitting for a square antiprism geometry (Fig. 2b). A summary table for the geometry calculation is given in Table S3. Regarding to the ligands in (**2**), the coordination mode observed for oxalate anion correspond to μ_2-$\kappa O,O'$-$\kappa O''O'''$ binding two Gd^{III} centres. In the case of IDC^{3-} anion, the coordination mode can be described as η^2-$\kappa N,O$-$\kappa O,O'$. The free carboxylate group is weakly interacting with a copper centre from a neighbouring layer with a Cu···O1 distance of 2.577(5) Å. The coordination of both IDC^{3-} and oxalate ligands are shown in Fig. 2c.

The 2D covalent structure of (**2**) can be described in terms of two homometallic fragments, Gd-based chains and Cu molecular moieties. In the Gd-chains, the diacuogadolinium centres are bonded by bis-chelating O,O'-oxalate anions to give $[Gd(H_2O)_2(C_2O_4)]^+$ moiety with $d_{Gd-Gd\#2}$ = 6.171(1) Å (#2 = $-x+1$, $-y+1$, $-z+2$) and $d_{Gd-Gd\#1}$ = 6.252(1) Å (#1 = $-x$, $-y+2$, $-z+2$). The inversion centre localized in the C=C bond belonging to the oxalate ion (C6—C6$^{\#1}$, #1 = $-x$, $2-y$, $2-z$) define the zigzag chains, which are disposed in a parallel form along the *ab* plane. In the $[Cu(IDC)]^-$ fragments, two carboxylate groups are acting as coordinating centres. The 2D covalent structure is reached by the coordination of the Gd chains with the $[Cu(IDC)]^-$ moieties (Fig. 3a) through both carboxylate groups, one in a monodentate fashion and the second bridging the 3*d* and 4*f* cations, with a $d_{Gd-Gd\#4}$ = 6.289(1) Å (#4 = x, $y+1$, z). A 3D structure is reached by hydrogen bonding interactions between the layers (O—H···O, Table 2) and also for pseudo coordinative axial interaction between carboxylate groups of one layer and Cu^{II} cations of a neighbouring layer (Cu···O1 distance of 2.577(5) Å). Gd···Cu#4 interlayer inter-

Table 1
Crystal data for (**1**) and (**2**).

	1	**2**
Formula	$CuC_{20}H_{18}N_6O_{10}$	$CuGdC_7H_7O_{11}N_2$
MM/g mol^1	565.9	515.96
T (K)	298	298
Crystal System	triclinic	triclinic
Space group	$P\bar{1}$	$P\bar{1}$
a/Å	7.720(7)	6.964(2)
b/Å	13.086(11)	7.159(2)
c/Å	14.329(13)	12.180(4)
α/°	92.821(15)	101.904(3)
β/°	103.940(15)	91.500(4)
γ/°	106.471(17)	94.031(4)
V/$Å^{-3}$	1336.5	592.194
Z	17	5
R-factor (%)	–	4.1

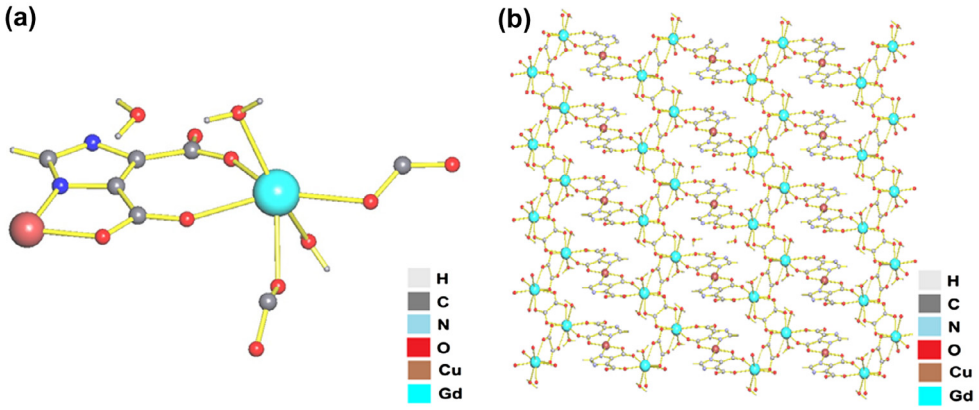

Fig. 1. (a) Asymmetric unit and (b) *ac* plane view of extended structure of (**2**).

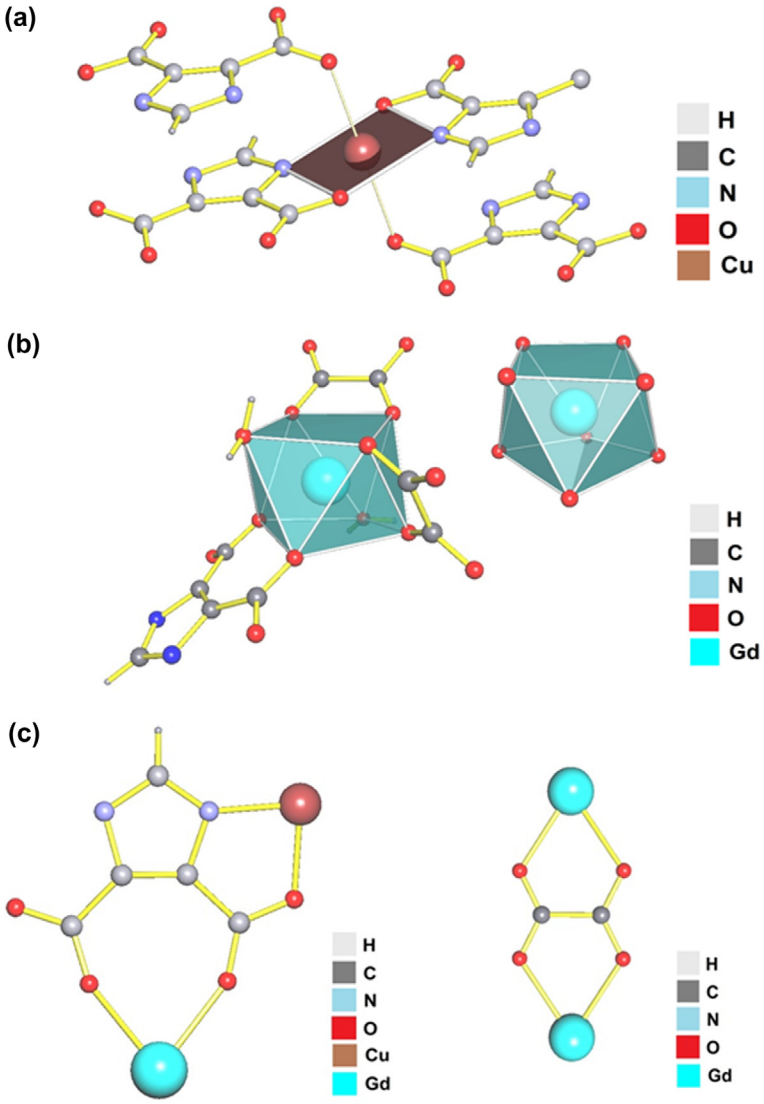

Fig. 2. Coordination environment and geometry for (a) Cu^{II}, (b) Gd^{III} and (c) coordination modes for IDC^{3-} and $C_2O_4^{2-}$ in (**2**).

actions through *syn–anti* carboxylate ligands can be also defined, with a distance of 5.517(13) Å (#4 = *x*, *y* + 1, *z*). The simplification of the network by a contraction of IDC^{3-} and $C_2O_4^{2-}$ to its respective centroids, gives a ditopic angular and lineal spacer respectively, while the Cu^{II} and Gd^{III} centres give a two and three connected nodes, respectively (Fig. 3b). This simplification permits to identify more clearly the zigzag Gd-chains and the connections by the Cu-isolated fragments.

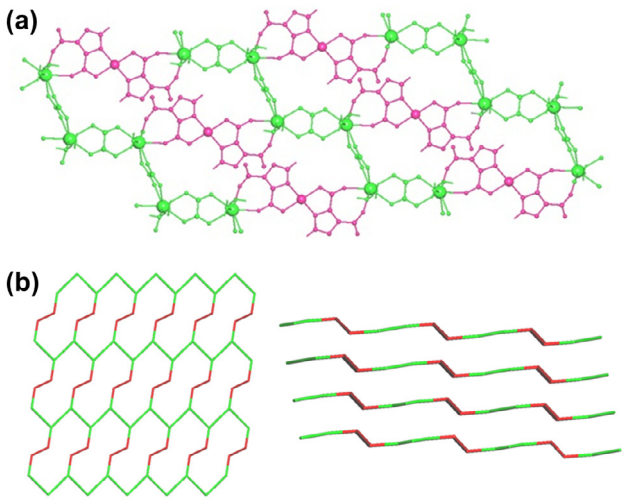

Fig. 3. (a) View of the 2D covalent structure of (**2**), in fuchsia the $[Cu(IDC)]^-$ moieties and in green the $[Gd(H_2O)_2(C_2O_4)]^+$ zigzag chains. (b) Simplified view of the extended structure of (**2**); Gd-chains in green and Cu-moieties in red. (Colour Online.)

Is important to state that in the Cambridge Data Base no results were obtained for Cu^{II}–Gd^{III} heterometallic systems based on the H_3IDC ligand. However, three similar systems can be found for triazole and pyrazole: $[Cu_2Gd(TDA)_2N_3(H_2O)_4{\cdot}2H_2O]$ [40], $[Cu_2Gd(TDA)_2\text{-}Cl(H_2O)_4]{\cdot}2H_2O$ [41] and $[CuLn_2(pdc)_2(SO_4)(H_2O)_4]{\cdot}H_2O$ [42] where H_2TDA is 1,2,3-triazole-4,5-dicarboxylic acid and H_3pdc is 3,5-pyrazoledicarboxylic acid. The two compounds based on triazole were synthesized under hydrothermal conditions and correspond to 3D networks, where the TDA^{2-} presents a κ*N*,*O*-, κ*O*,*O*′ for Cu^{II} and Gd^{III}, respectively similar to the observed for IDC^{3-} in (**2**). The main difference between these compounds is the presence of N_3^- or Cl^- as auxiliary ligands. The third example also corresponds to a 3D network obtained from 3,5-pyrazoledicarboxylate (pdc^{3-}) and SO_4^{2-} anion as ligands. In this case, the coordination mode of the pdc^{3-} anion is κ*O*,*N* for the Cu^{II} cation and κ*N*′,*O*′-κ*O*″,*O*‴ for the Gd^{III} cation, being the last coordination mode different to the observed in (**2**).

Taking into account the lack of similar reported Cu^{II}–Gd^{III} heterometallic compounds, we compare the structural characteristics of (**2**) with two previously reported Co^{II}–Gd^{III} 3D heterometallic networks synthesized also with H_3IDC and oxalate as ligands [28]. In these 3*d*-Gd^{III} networks independent substructures formed by Gd^{III}-oxalate can be identified, which are connected to each other by 3*d* moieties, Co^{II}-$HIDC^{2-}$/IDC^{3-} based zigzag chiral chains in Co^{II}–Gd^{III} networks and Cu^{II}–IDC^{3-} isolated moieties in (**2**). This difference could be originated by the spatial disposition of the $HIDC^{2-}$/IDC^{3-} ligands, being *trans* in the Co^{II} chains and *cis* in the Cu^{II} molecules, together with the coordination geometry that each metal centres can acquire (octahedral CoN_2O_4 and square plane CuN_2O_2). On the other hand, the coordination of IDC^{3-} is η^4-κ*N*,*O*-κ*O*,*O*′-κ*O*′,*O*″-κ*O*‴,*N* for Co^{II}–Gd^{III} networks and η^2-κ*N*,*O*-κ*O*,*O*′ for the Cu^{II}–Gd^{III} network (**2**). Furthermore, the Co^{II}–Gd^{III} networks are characterised by having Gd–Gd connected by 1,1-carboxylate and oxalate bridges, while Co–Gd cations are connected either by 1,1 and 1,3-carboxylate bridges, being the last one in an *anti–anti* conformation. However, in the case of compound (**2**) the Gd–Gd atoms are only bridged by oxalate groups and the Cu–Gd cations are only connected by one 1,3-carboxylate bridge with an *anti–anti* conformation.

Since small modifications in the hydro/solvothermal conditions can produce great structural and compositional changes, the higher metal condensation degree observed in the Co^{II}–Gd^{III} network is not surprising. Literature data show some studies that correlate the condensation of metal centres around of the carboxylates groups with the used temperature in the hydrothermal synthesis. Thus, the work reported by Chen et al. [43], and Tong et al. [44], show that under hydrothermal conditions, a higher reaction temperature should favour a higher diversity of the coordination modes of the carboxylate groups together with a higher amount of metal cations coordinated to these groups. Therefore, it seems reasonable to consider that the higher temperature used to obtain both Co^{II}–Gd^{III} networks (165 and 170 °C) compared with the used in (**2**) (120 °C), should explain the lesser metal content.

4.5. Magnetic properties

The *dc* magnetic measurements using a polycrystalline sample of (**2**) were performed as function of magnetic field and temperature. The temperature dependence of magnetic susceptibility was obtained between 2 and 300 K at applied fields of 0.2, 0.5 and 1 kOe; $\chi_M T$ versus T plots are shown in Fig. 4. For the three applied fields, a similar behaviour was observed between room temperature and 20 K. The $\chi_M T$ value at room temperature is near to 8.4 emuKmol^{-1}, slightly higher than the expected for non-interacting centres of Cu^{II} and Gd^{III} (8.25 emuKmol^{-1}; $S_{Cu} = 1/2$, $S_{Gd} = 7/2$ and $g = 2$). A higher $\chi_M T$ value at room temperature has been also reported for other 3D-heterometallic networks based on Cu^{II}–Gd^{III} [45]. As the sample is cooled down, $\chi_M T$ values remain constant till 100 K. Between 100 and 20 K, a slight decrease of $\chi_M T$ can be observed, reaching a value of 8.1 emuKmol^{-1} at 20 K, indicating that antiferromagnetic interactions predominate in this temperature range. Below 20 K, the $\chi_M T$ values become dependent of the applied field and an abrupt increase of $\chi_M T$ is evidenced. For the lowest applied field of 0.2 kOe a constant increase of $\chi_M T$ is observed until a value of 10.0 emuKmol^{-1} is reached at 2 K. However, a maximum value of the $\chi_M T$ is observed at applied fields of 0.5 and 1.0 kOe. For an applied field of 0.5 kOe, the maximum value of 9.2 emuKmol^{-1} is reached at 3.4 K while for 1.0 kOe the maximum of 8.6 emuKmol^{-1} is observed at 6.5 K. Below this maximum temperature, the $\chi_M T$ values decrease again reaching at 2 K values of 8.9 and 6.7 emuKmol^{-1} for 0.5 kOe and 1.0 kOe, respectively. The increase of $\chi_M T$ value below 20 K is indicative that in this temperature range ferromagnetic interactions are present. In addition, the χ_M^{-1} versus T plot at 0.2 kOe follows the Curie–Weiss law between 300 and 50 K. The fitting of the experimental data gives a θ value of −0.08 K and C = 8.4 emuKmol^{-1} (Fig. S5). The negative

Table 2
Hydrogen bonds for (**2**).

D—H···A	d(D—H)	d(H···A)	d(D···A)	<(DHA)
O(9)—H(9A)···O(4)#4	0.849(9)	1.940(13)	2.787(6)	175(7)
O(9)—H(9B)···O(6)#5	0.849(9)	2.05(3)	2.856(6)	157(7)
O(10)—H(10A)···O(8)#6	0.848(9)	2.027(11)	2.874(6)	178(7)
O(10)—H(10B)···O(11)	0.847(9)	1.83(3)	2.640(6)	160(7)
O(11)—H(11B)···O(1)#7	0.849(9)	2.04(4)	2.804(7)	149(7)

#1 −*x*, −*y* + 2, −*z* + 2, #2 −*x* + 1, −*y* + 1, −*z* + 2, #3 −*x* + 1, −*y*, −*z* + 1, #4*x*, *y* + 1, *z*, #5*x* + 1, *y*, *z*, #6*x* − 1, *y*, *z*, #7−*x*, −*y* + 1, −*z* + 1.

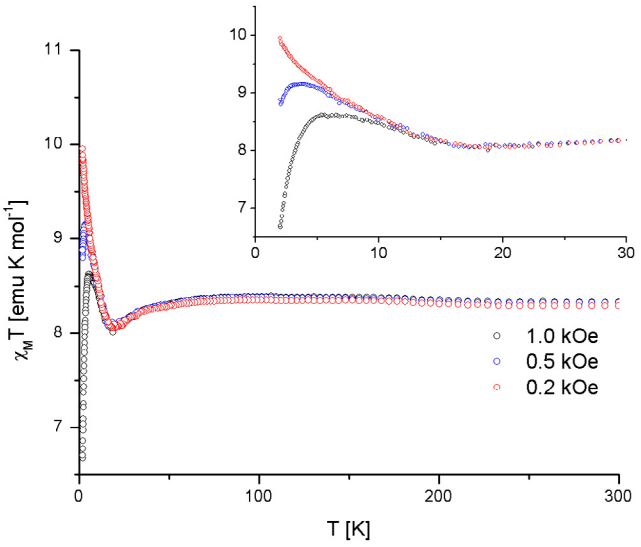

Fig. 4. χ_MT vs. T plot for (**2**) at applied fields of 0.2, 0.5 and 1.0 kOe.

Weiss constant is indicative that the bulk interaction between the metal centres is weakly antiferromagnetic in nature.

The field dependence of the reduced magnetization of (**2**) at 11, 9, 7, 5, 3 and 2 K are given in Fig. 5a. According with these data, the saturation of (**2**) is reached at approximately 60 kOe only at 2 and 3 K, giving a value of 8.0 N_β, which correlates well with that expected for eight electrons (one electron of Cu^{II}-d^9 and seven of Gd^{III}-f^7). Furthermore, the N_β versus HT^{-1} plots at different temperatures show a complete overlap of the curves, thus confirming the lack of first-order orbital moment contribution. To corroborate the existence of a magnetic order at low temperatures, isothermal magnetic hysteresis loops were measured at 2, 3 and 4 K between ±60 kOe (Fig. 5b). Although the coercivity field (H_c) and remnant magnetization (M_r) were observed for all isothermal hysteresis loops, higher values of H_c and M_r of 50 Oe and 500 emumol^{-1} were observed at 2 K. Additionally, alternating current (*ac*) magnetic susceptibility measurements between 1.8 and 22 K were performed on (**2**). Although *ac* susceptibilities are very small and noisy, a maximum near to 10 K can be found both the in-phase (χ'_M) and out-of-phase (χ''_M) susceptibility (Fig. S6), which is in agreement with the *dc* susceptibility data. Finally, both the in-phase (χ'_M) and out-of-phase (χ''_M) maximum is frequency independent.

Besides, the inter-layer interactions through Cu^{II}–Cu^{II} and Cu^{II}–Gd^{III} cations together with the presence of a hetero-spin system (S_{Cu} = 1/2; S_{Gd} = 7/2), makes the analysis of magnetic behaviour more complex (Fig. 6). It is important to note that the interactions between the Gd^{III} cations occur exclusively by oxalate bis-chelating bridges with a length of ca. 6 Å, being similar to those reported by Cañadillas et al., for Gd-oxalate honeycomb-2D networks, where a very weak antiferromagnetic coupling between the Gd^{III} cations was observed ($J = -0.005$ cm^{-1}) [46]. The Gd–Cu interactions present in (**2**) are mediated by *anti–anti* or *syn–anti* carboxylate bridges, belonging to intralayer o interlayer interactions, respectively. Literature data show that analogous 1D systems presenting Cu^{II}–Gd^{III} bonded by *syn–anti* carboxylate bridges and with a Cu···Gd distance of 5.991 Å, have a ferromagnetic interaction between the metal centres, giving a *J* value of 1.3 cm^{-1} [12]. The same type of magnetic interactions ($J = 0.426$ cm^{-1}) was also reported for 3D Cu^{II}–Gd^{III} networks, with Cu···Gd distance of 6.010 Å and bonded by *anti–anti* carboxylate bridges [47]. Another magnetic pathway correspond to the IDC^{3-} anion, with both carboxylate groups permitting the interlayer communication of the copper(II) cations via axial-equatorial interactions. In this sense, Ghoshal et al., report for analogous systems that the interaction between copper(II) cations depends of the axial Cu—O distances, giving smaller *J* values for longer axial distances. Furthermore the authors also reported that the succinate ligand, which is similar to the Cu—O_2CCCCO_2—Cu fragment of the IDC^{3-}, produces an antiferromagnetic coupling between copper(II) centres, with a *J* value of −2.7 cm^{-1} [48]. Table 3 summarizes the structural characteristics of each exchange pathway present in (**2**). Taking into account all the above-mentioned behaviour the antiferromagnetic interactions observed for (**2**), should arise from the Gd–Gd and Cu–Cu interactions, while the Cu–Gd interactions should be responsible for the ferromagnetic interactions.

5. Conclusions

In summary, a new Cu^{II}–Gd^{III} heterometallic coordination polymer was obtained using a two-step synthesis, where the previously synthesized mononuclear complex $[Cu(H_2IDC)_2(2,2bipy)]\cdot 2H_2O$ acts as a metalloligand. The assembly of the mononuclear complex to give the extended network $[Gd(H_2O)_2(C_2O_4)Cu(IDC)]\cdot H_2O$ is reached under hydrothermal conditions, being promoted by the incorporation of an auxiliary ligand (oxalate) and a 4*f* cation. Clearly, the experimental conditions used in this work, together

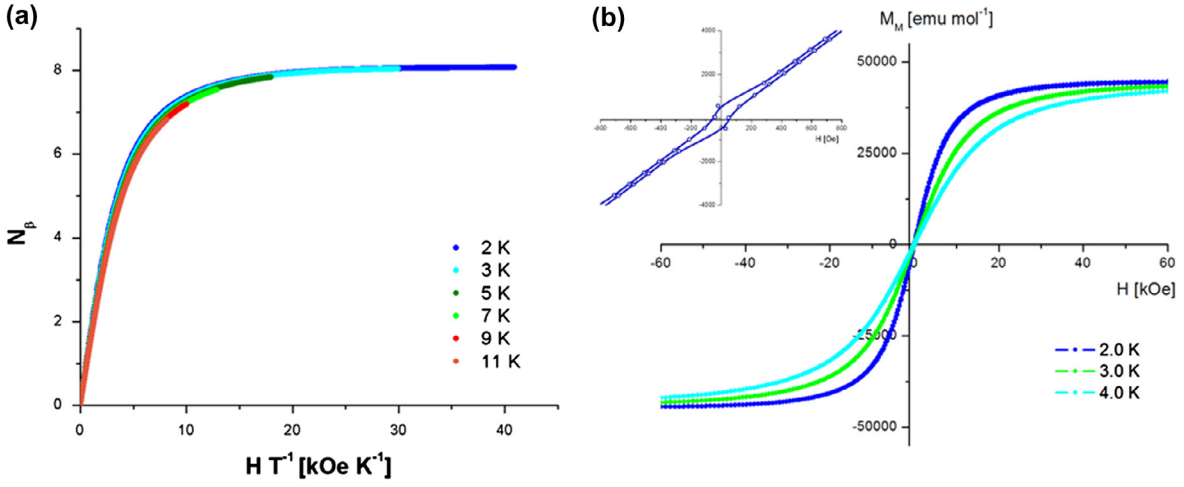

Fig. 5. (a) N_β vs. HT^{-1} curves for (**2**), measured at 11, 9, 7, 5, 3 and 2 K. (b) Hysteresis loop of (**2**) at 2, 3 and 4 K, with an inset for the 2 K loop.

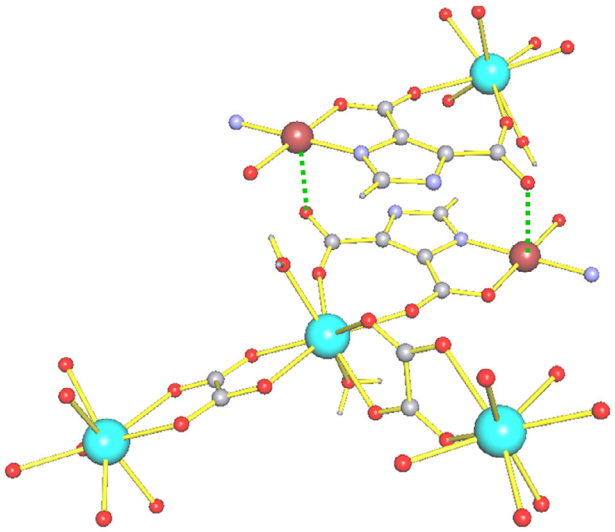

Fig. 6. Types of bridges found in the extended structure of (**2**); in green the interactions that result from the interlayer packing. (Colour Online.)

Table 3
Summary of bridges involved in (**2**).

Connection	Bridge type	Distance (Å)
Gd1–Gd1#2	oxalate	6.171(1)
Gd1–Gd1#1	oxalate	6.252(1)
Gd1–Cu1#4	carboxylate *anti–anti*	6.289(1)
Gd1–Cu1#4	carboxylate *syn–anti*[*]	5.517(13)
Cu1–Cu1#4	imidazolate[*]	7.159(2)

#1 $-x, -y+2, -z+2$, #2 $-x+1, -y+1, -z+2$, #3 $-x+1, -y, -z+1$, #4 $x, y+1, z$ #5 $x+1, y, z$, #6 $x-1, y, z$, #7 $-x, -y+1, -z+1$.

[*] Interactions that result from the interlayer packing.

with the choice of a ligand with multiple deprotonation degrees and the wide capability to bind multiples metal centres, offers an excellent synthetic approach to obtain novel 3*d*–4*f* heterometallic compounds. This Cu^{II}–Gd^{III} network is one of the few reported 3*d*–4*f* coordination polymers based on the 1H-imidazole-4,5-dicarboxylic acid (H_3IDC) ligand. The 2D lamellar structure of $[Gd(H_2O)_2(C_2O_4)Cu(IDC)]\cdot H_2O$ is reached by the link of 1D-zigzag Gd-chains and discreet Cu^{II} complexes. A 3D structure is reached by hydrogen bonding interactions and the axial interaction between carboxylate groups and Cu^{II} cations belonging to two parallel sheets. Also Gd···Cu interlayer interactions through *syn–anti* carboxylate ligands can be established. From a magnetic point of view, the experimental evidence shows that the Cu^{II}–Gd^{III} network behaves as paramagnet from room temperature to 100 K and antiferromagnet between 100 and 20 K. But the most important aspect, is the ferromagnetic behaviour observed at low temperatures.

Acknowledgements

The authors acknowledge financial support from FONDECYT 1130643, Proyecto Anillo CONICYT ACT 1404, CONICYT-FONDEQUIP/PPMS/EQM130086, and to the International collaborative projects LIA-MIF 836 and ECOS/CONICYT C15E02. The authors are also members of CEDENNA, Financiamiento Basal, FB0807. C.Cruz, thanks CONICYT Fellowship 2114042.

Appendix A. Supplementary data

CCDC 1524660 contains the supplementary crystallographic data for (**2**). These data can be obtained free of charge via http://www.ccdc.cam.ac.uk/conts/retrieving.html, or from the Cambridge Crystallographic Data Centre, 12 Union Road, Cambridge CB2 1EZ, UK; fax: (+44) 1223-336-033; or e-mail: deposit@ccdc.cam.ac.uk.

Supplementary data associated with this article can be found, in the online version, at http://dx.doi.org/10.1016/j.poly.2017.02.002.

References

[1] D. Aulakh, J.B. Pyser, X. Zhang, A.A. Yakovenko, K.R. Dunbar, M. Wriedt, Metal-organic frameworks as platforms for the controlled nanostructuring of single-molecule magnets, J. Am. Chem. Soc. 137 (2015) 9254–9257, http://dx.doi.org/10.1021/jacs.5b06002.
[2] W.P. Lustig, F. Wang, S.J. Teat, Z. Hu, Q. Gong, J. Li, Chromophore-based luminescent metal-organic frameworks as lighting phosphors, Inorg. Chem. 55 (2016) 7250–7256, http://dx.doi.org/10.1021/acs.inorgchem.6b00897.
[3] A.H. Chughtai, N. Ahmad, H.A. Younus, A. Laypkov, F. Verpoort, Metal-organic frameworks: versatile heterogeneous catalysts for efficient catalytic organic transformations, Chem. Soc. Rev. 44 (2015) 6804–6849, http://dx.doi.org/10.1039/c4cs00395k.
[4] J.A. Mason, M. Veenstra, J. Long, Evaluating metal–organic frameworks for natural gas storage, Chem. Sci. 5 (2014) 32–51, http://dx.doi.org/10.1039/c3sc52633j.
[5] J. Li, Y. Ma, M.C. Mccarthy, J. Sculley, J. Yu, H. Jeong, P.B. Balbuena, H. Zhou, Carbon dioxide capture-related gas adsorption and separation in metal-organic frameworks, Coord. Chem. Rev. 255 (2011) 1791–1823, http://dx.doi.org/10.1016/j.ccr.2011.02.012.
[6] X. Tan, Y. Du, Y. Che, J. Zheng, Syntheses, structures and magnetic properties of one family of 3d–4f chiral metal-organic frameworks (MOFs) based on D (+)-camphoric acid, Inorg. Chem. 36 (2013) 63–67, http://dx.doi.org/10.1016/j.inoche.2013.08.012.
[7] M. Andruh, J. Costes, C. Diaz, S. Gao, 3d–4f combined chemistry: synthetic strategies and magnetic properties, Inorg. Chem. 48 (2009) 3342–3359, http://dx.doi.org/10.1021/ic801027q.
[8] G. Zeng, S. Xing, X. Wang, Y. Yang, D. Ma, H. Liang, L. Gao, J. Hua, G. Li, Z. Shi, S. Feng, 3d–4f metal-organic framework with dual luminescent centers that efficiently discriminates the isomer and homologues of small organic molecules, Inorg. Chem. 55 (2016) 1089–1095, http://dx.doi.org/10.1021/acs.inorgchem.5b02193.
[9] S. Zhang, P. Cheng, Recent advances in the construction of lanthanide- copper heterometallic metal-organic frameworks, CrystEngComm 17 (2015) 4250–4271, http://dx.doi.org/10.1039/C5CE00237K.
[10] J.L. Sanz, R. Ruiz, A. Gleizes, F. Lloret, J. Faus, M. Julve, J.J. Borrás-Almenar, Y. Journaux, Crystal structures and magnetic properties of novel [Ln(III)Cu(II)(4)] (Ln = Gd, Dy, Ho) pentanuclear complexes. Topology and ferromagnetic interaction in the Ln(III)-Cu(II) Pair, Inorg. Chem. 35 (1996) 7384–7393, http://dx.doi.org/10.1021/ic960524t.
[11] R. Ruiz, J. Faus, F. Lloret, M. Julve, Y. Journaux, Coordination chemistry of N, N'-bis(coordinating group substituted)oxamides: a rational design of nuclearity tailored polynuclear complexes, Coord. Chem. Rev. 193–195 (1999) 1069–1117, http://dx.doi.org/10.1016/S0010-8545(99)00138-1.
[12] Y. Zou, F. Yin, X.J. Zhou, J. Chen, Q.J. Meng, A CuII-GdIII-CuII heterometallic coordination polymer constructed by gadolinium(III) ion and copper(II) Schiff-base building block: structure and magnetic property, Inorg. Chem. Commun. 45 (2014) 25–29, http://dx.doi.org/10.1016/j.inoche.2014.03.045.
[13] K.F. Konidaris, C.N. Morrison, J.G. Servetas, M. Haukka, Y. Lan, A.K. Powell, J.C. Plakatouras, G.E. Kostakis, Supramolecular assemblies involving metal-organic ring interactions: heterometallic Cu(II)-Ln(III) two-dimensional coordination polymers, CrystEngComm 14 (2012) 1842–1849, http://dx.doi.org/10.1039/c2ce06180e.
[14] J.W. Ye, Y. Liu, Y.F. Zhao, X.Y. Mu, P. Zhang, Y. Wang, Porous lanthanide-copper coordination frameworks exhibiting reversible single-crystal-to-single-crystal transformation based on variable coordination number and geometry, CrystEngComm 10 (2008) 598–604, http://dx.doi.org/10.1039/b712280b.
[15] X.H. Miao, S. De Han, S.J. Liu, X.H. Bu, Two lanthanide(III)-copper(II) chains based on [Cu2Ln 2] clusters exhibiting high stability, magnetocaloric effect and slow magnetic relaxation, Chin. Chem. Lett. 25 (2014) 829–834, http://dx.doi.org/10.1016/j.cclet.2014.05.025.
[16] Z.G. Gu, H.C. Fang, P. yi Yin, L. Tong, Y. Ying, S.J. Hu, W.S. Li, Y.P. Cai, A family of three-dimensional lanthanide-zinc heterometal-organic frameworks from 4,5-imidazoledicarboxylate and oxalate, Cryst. Growth Des. 11 (2011) 2220–2227, http://dx.doi.org/10.1021/cg1015753.
[17] S.M. Li, X.J. Zheng, D.Q. Yuan, A. Ablet, L.P. Jin, In situ formed white-light-emitting lanthanide-zinc-organic frameworks, Inorg. Chem. 51 (2012) 1201–1203, http://dx.doi.org/10.1021/ic201425v.
[18] SAINTPLUS, V6.22; Bruker AXS Inc: Madison, WI, USA, 2000, (2000).
[19] SADABS, V2.05; Bruker AXS Inc.: Madison, WI, USA, 2001, (2001).
[20] O.V. Dolomanov, L.J. Bourhis, R.J. Gildea, J.A.K. Howard, H. Puschmann, OLEX2: a complete structure solution, refinement and analysis program, J. Appl. Crystallogr. 42 (2009) 339–341, http://dx.doi.org/10.1107/S0021889808042726.
[21] G.M. Sheldrick, SHELXT - Integrated space-group and crystal-structure determination, Acta Crystallogr. A A71 (2015) 3–8, http://dx.doi.org/10.1107/S2053273314026370.

[22] G.M. Sheldrick, Crystal structure refinement with SHELXL, Acta Crystallogr., Sect. C: Cryst. Struct. Commun. C71 (2015) 3–8, http://dx.doi.org/10.1107/S2053229614024218.
[23] G.A. Bain, J.F. Berry, Diamagnetic corrections and pascal's constants, J. Chem. Educ. 85 (2008) 532–536, http://dx.doi.org/10.1021/ed085p532.
[24] W. Lu, D. Zhong, L. Jiang, T. Lu, Lanthanide coordination polymers constructed from imidazole-4,5- dicarboxylate and sulfate: syntheses, structural diversity, and photoluminescent properties, Cryst. Growth Des. 12 (2012) 3675–3683, http://dx.doi.org/10.1021/cg300476e.
[25] Z. Li, Z. Zhang, J. Dai, H. Huang, X. Li, S. Yue, Y. Liu, Three novel lanthanide complexes with imidazole-4, 5-dicarboxylate ligand: Hydrothermal syntheses, structural characterization, and properties, J. Mol. Struct. 963 (2010) 50–56, http://dx.doi.org/10.1016/j.molstruc.2009.10.009.
[26] L. Zhu, Y. Zhao, S. Yu, M. Zhao, Construction of two 2D 3d–4f coordination complexes based on the linkages of left-and right-handed helical chains, Inorg. Chem. 13 (2010) 1299–1303, http://dx.doi.org/10.1016/j.inoche.2010.07.021.
[27] Y. Ding, T. Li, X. Hong, L. Zhu, Y. Cai, S. Zhu, S. Yu, Construction of four 3d–4f heterometallic pillar-layered frameworks containing left- and right-handed helical chains and a I− chemosensor, CrystEngComm 12 (2015) 3945–3952, http://dx.doi.org/10.1039/C5CE00324E.
[28] C. Cruz, E. Spodine, A. Vega, D. Venegas-Yazigi, V. Paredes, Garcia, novel 3d/4f Metal organic networks containing Co(II) chiral chains, Cryst. Growth Des. 16 (2016) 2173–2182, http://dx.doi.org/10.1021/acs.cgd.5b01843.
[29] F. M. de, Ó.A. de Moura, R.F. de Oliveira, de Farias, Synthesis, characterization and thermogravimetric study of zinc group halides adducts with imidazole, Thermochim. Acta 405 (2003) 219–224, http://dx.doi.org/10.1016/S0040-6031(03)00191-6.
[30] X. Feng, Y. Feng, J.J. Chen, S. Ng, L. Wang, J. Guo, Reticular three-dimensional 3d–4f frameworks constructed through substituted imidazole-dicarboxylate: syntheses, luminescence and magnetic properties study, Dalton Trans. 44 (2014) 804–816, http://dx.doi.org/10.1039/c4dt02047b.
[31] W. Manch, W.C. Fernelius, The structure and spectra of nickel(II) and copper(II) complexes, J. Chem. Educ. 38 (1961) 192–201, http://dx.doi.org/10.1021/ed038p192.
[32] S. Kongchoo, A. Kantacha, S. Saithong, S. Wongnawa, Synthesis, crystal structure, and spectroscopic properties of Cu(II) complex with 14-membered hexaazamacrocyclic ligands, J. Chem. Crystallogr. 46 (2016) 222–229, http://dx.doi.org/10.1007/s10870-016-0649-8.
[33] S.L. Reddy, T. Endo, G.S.R. Reddy, Electronic (absorption) spectra of 3d transition metal complexes, Adv. Aspects Spectrosc. (2012) 3–48, http://dx.doi.org/10.5772/50128.
[34] L.-Z. He, S.-J. Li, W.-D. Song, D.-L. Miao, Diaquabis(1H-imidazole-4-carboxylato-κ2N3, O)-cobalt(II), Acta Crystallogr., Sect. E: Struct. Rep. Online 68 (2012), http://dx.doi.org/10.1107/S1600536812037579, m1246–m1246.
[35] D.-C. Zhong, H.-B. Guo, J.-H. Deng, P. Lian, X.-Z. Luo, A two-dimensional copper (II) coordination polymer based on 2-propyl-1 *H* -imidazole-4,5-dicarboxylic acid, Acta Crystallogr., Sect. C: Cryst. Struct. Commun. 71 (2015) 152–154, http://dx.doi.org/10.1107/S2053229615000546.
[36] D.-P. Wang, Y.-G. Chen, H.-Y. Wang, C.-J. Zhang, Q. Tang, Syntheses, crystal structures, and properties of four new coordination compounds of transition metals and imidazoledicarboxylic acid derivatives, J. Coord. Chem. 64 (2011) 2824–2833, http://dx.doi.org/10.1080/00958972.2011.606907.
[37] E. Shimizu, M. Kondo, Y. Fuwa, R.P. Sarker, M. Miyazawa, M. Ueno, T. Naito, K. Maeda, F. Uchida, Synthesis and crystal structures of metal complexes with 4,5-imidazole-dicarboxylate chelates: self-assembled structures via NHEllipsis O=C intermolecular hydrogen bonds, Inorg. Chem. Commun. 7 (2004) 1191–1194, http://dx.doi.org/10.1016/j.inoche.2004.09.008.
[38] D.E. Wang, Z.F. Tian, F. Wang, L.L. Wen, D.F. Li, Syntheses and crystal structures of two inorganic-organic hybrid frameworks constructed from pyridine-2,5-dicarboxylic acid, J. Inorg. Organomet. Polym Mater. 19 (2009) 196–201, http://dx.doi.org/10.1007/s10904-008-9244-6.
[39] K. Shankar, A.M. Kirillov, J.B. Baruah, Bottom up synthesis for homo- and heterometallic 2,3-pyridinedicarboxylate coordination compounds, Polyhedron 102 (2015) 521–529, http://dx.doi.org/10.1016/j.poly.2015.10.031.
[40] X. Jiang, S.-D. Han, R. Zhao, J. Xu, X.-H. Bu, Ln III ion dependent magnetism in heterometallic Cu–Ln complexes based on an azido group and 1,2,3-triazole-4,5-dicarboxylate as co-ligands, RSC Adv. 5 (2015) 62319–62324, http://dx.doi.org/10.1039/C5RA07972A.
[41] J.-Y. Zou, N. Xu, W. Shi, H.-L. Gao, J.-Z. Cui, P. Cheng, A new family of 3d–4f heterometallic coordination polymers assembled with 1H–1,2,3-triazole-4,5-dicarboxylic acid: syntheses, structures and magnetic properties, RSC Adv. 3 (2013) 21511–21516, http://dx.doi.org/10.1039/c3ra43118e.
[42] X.-H. Zhou, Y.-H. Peng, X.-D. Du, C.-F. Wang, J.-L. Zuo, X.-Z. You, New 3d–4f heterometallic coordination polymers based on pyrazole-bridged Cu II Ln III dinuclear units and sulfate anions: syntheses, structures, and magnetic properties, Cryst. Growth Des. 9 (2009) 1028–1035, http://dx.doi.org/10.1021/cg800848n.
[43] J. Chen, M. Ohba, D. Zhao, W. Kaneko, S. Kitagawa, Polynuclear core-based nickel 1,4-cyclohexanedicarboxylate coordination polymers as temperature-dependent hydrothermal reaction products, Cryst. Growth Des. 4 (2006) 664–668, http://dx.doi.org/10.1021/cg050363g.
[44] M.-L. Tong, S. Hu, J. Wang, S. Kitagawa, S.W. Ng, Supramolecular isomerism in cadmium hydroxide phases. temperature-dependent synthesis and structure of photoluminescent coordination polymers of a- and b-Cd2(OH)2(2,4-pyda), Cryst. Growth Des. 2 (2005) 4–6, http://dx.doi.org/10.1021/cg049610r.
[45] J. Xu, W. Su, M. Hong, 3D lanthanide-transition-metal-organic frameworks constructed from tetranuclear Ln4 SBUs and Cu centres with fsc net, CrystEngComm 13 (2011) 3998–4004, http://dx.doi.org/10.1039/c0ce00800a.
[46] L. Cañadillas-Delgado, J. Pasan, O. Fabelo, M. Hernandez-Molina, F. Lloret, M. Julve, C. Ruiz-Pérez, Two- and three-dimensional networks of gadolinium(III) with dicarboxylate ligands: synthesis, crystal structure, and magnetic properties, Inorg. Chem. 45 (2006) 10585–10594, http://dx.doi.org/10.1021/ic061173d.
[47] S. Liu, W. Song, L. Xue, S. Han, Y. Zeng, L. Wang, X. Bu, Three new Cu(II)-Ln(III) heterometallic coordination polymers constructed from quinolinic acid and nicotinic acid: synthesis, structures, and magnetic properties, Sci. China Chem. 55 (2012) 1064–1072, http://dx.doi.org/10.1007/s11426-012-4590-1.
[48] D. Ghoshal, T.K. Maji, G. Mostafa, S. Sain, T.-H. Lu, J. Ribas, E. Zangrando, N.R. Chaudhuri, Polymeric networks of copper(II) using succinate and aromatic N-N donor ligands: synthesis, crystal structure, magnetic behaviour and the effect of weak interactions on their crystal packing, Dalton Trans. (2004) 1687–1695, http://dx.doi.org/10.1030/b401738b.